Energy migration of the local excitation at the Eu^{3+} site in a Eu–O chemical cluster in sol-gel derived SiO_2:Eu^{3+} glasses

Tomokatsu Hayakawa[a] and Masayuki Nogami
Department of Materials Science and Engineering, Nagoya Institute of Technology, Gokiso, Showa, Nagoya, Aichi 466-8555, Japan

(Received 31 August 2000; accepted for publication 14 May 2001)

By using the fluorescence line-narrowing technique, we observed a broad fluorescence band in the vicinity of a resonant line of the $^5D_0 \rightarrow {}^7F_0$ transition in an Eu^{3+}-doped SiO_2 glass synthesized by a sol-gel process. The comparison with a similar line in an $Al_2O_3-SiO_2$:Eu^{3+} sol-gel glass revealed the existence of a chemical cluster of Eu^{3+} and O^{2-} in the tetrahedral SiO_4 network. The broad fluorescence band was attributable to an energy migration among the Eu^{3+} ions for the site-selectively received excitation energy. Also, based on Yokota–Tanimoto's energy diffusion model, the fluorescence decay curves for the $^5D_0 \rightarrow {}^7F_2$ transition were closely correlated with the energy migration and gel–glass transformation. The gel-shrinkage and reduced interatomic distance between Eu^{3+} ions due to a thermal treatment at higher temperature definitely resulted in a decrease in the associated lifetime of the initial decay. © *2001 American Institute of Physics.*
[DOI: 10.1063/1.1384491]

I. INTRODUCTION

Rare-earth doped glasses have attracted attention because of their optical properties such as laser oscillation,[1–3] up-conversion,[4] Faraday rotation,[5–7] and persistent spectral hole burning (PSHB).[8–10] These properties are a consequence of $4f$ electrons being shielded by the $5s$,$5p$ outer shells. The advantages in the utilization of a glass as a host material are its transparency, easy shape-forming, economical productivity, and a high incorporation density of rare-earth ions. Moreover, the manipulation of glass compositions can bring out the aforementioned functionalities for each application. Further development of such functional glasses requires detailed microscopic information, especially on the local structures around the rare-earth ions. Known as a high-resolution spectroscopy, a spectral hole burning method has been intensively applied in order to investigate local structures around optical centers.[11,12]

The formation of a spectral hole in a PSHB material containing rare-earth ions is accomplished by the following two processes: a local excitation at a rare-earth site by high-densified laser irradiation, and the generation of a ''hole'' at the corresponding frequency in the absorption spectrum which is inhomogeneously broadened by structural fluctuations. The observation of PSHB due to rare-earth ions was first reported by Jaaniso and Bill[13] who observed the persistence of a spectral hole at room temperature in $SrFCl_{0.5}Br_{0.5}$:Sm^{2+}. Hirao *et al.*[8,9] reported the persistent hole-burning in Sm^{2+}-doped borate and fluorohafnate glasses. Subsequently, Nogami[14] obtained PSHB observations in Sm^{2+}-doped $Al_2O_3-SiO_2$ glasses produced by a sol-gel method. From a practical point of view, PSHB is beneficial to high density data storage: One bit of datum is written as a ''hole'' in an absorption spectrum of optically activated ions or molecules. Ao[15] has estimated that a recording density of 10^9 bits/cm^2 could be realized on a conventional compact disk. This is just a three-dimensional data-storage including a frequency domain in addition to spatial two dimensions. Various types of Sm^{2+}-doped glasses have been synthesized as PSHB materials.[16] The main mechanism is believed to be the photoionization of Sm^{2+} to Sm^{3+} at room temperature. The processes for data-writing on absorption spectra were developed in such a way for two photon gate writing[17] or holography.[18]

Recently, Nogami *et al.* have succeeded in synthesizing Eu^{3+}-doped PSHB silica[19] and aluminosilicate[20] glasses using a sol-gel process. The new PSHB materials have the advantage that the reduction process for the valence states of rare-earth ions is not necessary, thus simplifying the synthesis process. He also reported curious line-narrowing spectra of the $^5D_0 \rightarrow {}^7F_1$ emissions in the sol-gel derived SiO_2:Eu^{3+} glass, the splitting of which appeared to be independent of the excitation energy. Similar findings of rare-earth fluorescence were reported by several researchers.[21,22] The sol-gel synthesis gives us an advantageous way to induce novel functionalities for optical materials. However, it is still not clarified what structures the resultant materials have and how they are interconnected with their optical functionalities.

Hereafter, we noted the photoluminescence of $98SiO_2-2Eu_2O_3$ glasses prepared by a sol-gel method. The optical data storage in the $98SiO_2-2Eu_2O_3$ glasses heated at 800 °C for 2 h in air could be accomplished above 77 K; the hole depth was ~10% and the hole width was ~2 cm^{-1} at 77 K when laser irradiation was 0.1 kW/cm^2 for 30 min. The spectral hole burnt at 77 K was persistent up to ~150 K.[19,23] This article will show experimental evidence for the existence of a europium–oxide chemical cluster in the SiO_2 glass, causing an energy migration among the Eu^{3+} sites. Localized energy or excitation propagated in disordered materials has created many arguments since Anderson's paper.[24]

[a]Electronic mail: hayatomo@mse.nitech.ac.jp

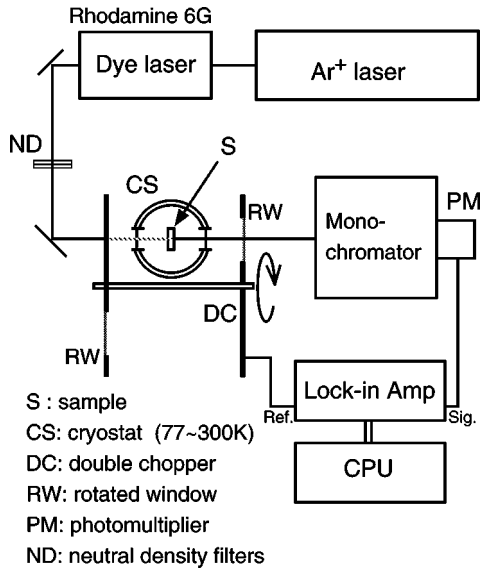

FIG. 1. Experimental setup for the measurement of the fluorescence around a resonant line of the $^5D_0 \rightarrow {}^7F_0$ transition in Eu^{3+}-doped glasses.

Chemical clustering of optical species in glasses might provide an ideal system for the investigation of Anderson's optical mobility edge.[25–27]

II. EXPERIMENT

We prepared three types of $98SiO_2-2Eu_2O_3$ glasses by calcining dry gels with the same composition in order to examine the influence of glass structures on the fluorescence properties of Eu^{3+}. The sample preparation of the $98SiO_2-2Eu_2O_3$ gels was described elsewhere.[19] The samples denoted as A800 and A1000 were heated at 800 and 1000 °C for 2 h in air, respectively. The AV800 sample was heated at 800 °C for 2 h in air and subsequently at 800 °C for 2 h in a vacuum. Raman spectroscopy was employed to distinguish the glass structures using a confocal type of Raman microprobe optics with a backscattering geometry (JASCO, NRS-2000). The magnification of the objective lens in the microscope component was ×20. The excitation source used in the Raman observation was the green line (514.5 nm) of an Ar^+ laser (NEC, GLS3280) with power of about 30 mW.

The fluorescence spectra were obtained using a tunable dye laser (Rhodamine 6G: 566–640 nm) pumped by an Ar^+ laser (Coherent, Innova 70). The dye laser could excite Eu^{3+} ions within the inhomogeneous absorption width of the $^7F_0 \rightarrow {}^5D_0$ transition. The experimental setup is shown in Fig. 1. A double chopper was used for measuring the resonant fluorescence of the $^5D_0 \rightarrow {}^7F_0$ transition. Special attention was paid to the optical alignment so as to insure that no scattered light disturbed the measurement of the resonant fluorescence of Eu^{3+} ions. Also, the output power of the dye laser was checked to be always invariable. The studies were carried out over the range of 77–300 K. Since the lifetime of the $^5D_0$ level was on the order of 10^{-3} s, the speed of the rotated chopper windows was appropriately controlled so as to produce the fluorescence within 0.2–2.0 ms immediately after the excitation light was mechanically chopped. The fluorescence was analyzed by a monochromator (spectral resolution $\sim 3.2\ cm^{-1}$) and detected with a photomultiplier. The signal was then processed and recorded by a lock-in amplifier controlled by a personal computer.

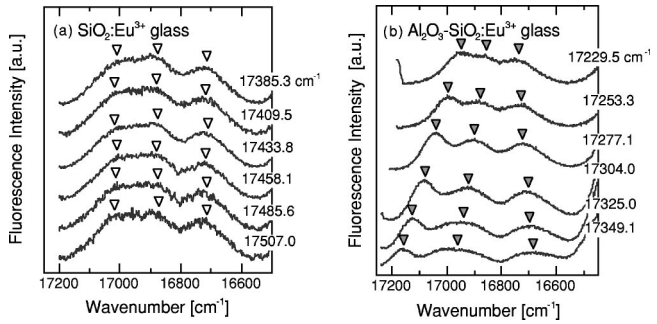

FIG. 2. Difference between the FLN spectra of $SiO_2:Eu^{3+}$ and $Al_2O_3-SiO_2:Eu^{3+}$ glasses, which were prepared by the sol-gel method: (a) SiO_2:5 wt %Eu_2O_3, heated at 800 °C for 2 h in air. (b) $10Al_2O_3-90SiO_2$:5 wt %Eu_2O_3, heated at 800 °C for 2 h in air. The wave number beside each FLN spectrum stands for the excitation energy.

We also measured the decay curves of the $^5D_0 \rightarrow {}^7F_2$ fluorescence after a pulsed excitation to the $^5D_0$ level with a Rhodamine 6G dye laser pumped by a N_2 laser (Laser Photonics, Inc., LN203C: pulse width ~1 ns). The fluorescence was led to a monochromator through an optical fiber and detected by an image-intensified charge-coupled device (ICCD) camera (Oriel Instruments, InstaSpec™V system). The exposure time of the ICCD camera was fixed at 10 μs. The delay time for the ICCD gate pulse was controlled from 0 to 3000 μs. The measurement of the fluorescence decay was performed at room temperature.

III. RESULTS

The fluorescence line-narrowing (FLN) technique is a powerful tool to obtain information on local structures around rare-earth ions in glasses and thus there has been an enormous number of investigations on rare-earth optics using the FLN technique.[28–32] Some of the results in our FLN measurements are exemplified in Fig. 2. Generally, $^5D_0 \rightarrow {}^7F_1$ emission lines are split into three components due to local fields around Eu^{3+} and their separations depend on the energy for the direct excitation from the $^7F_0$ ground level to the $^5D_0$ excited level. However, the splittings in the investigated $SiO_2:Eu^{3+}$ glasses appear to be independent of the variation in the excitation energy, as shown in Fig. 2(a). Even a 0.5–5 wt % concentration of Eu_2O_3 in SiO_2 glasses showed a similar behavior in each of the FLN spectra. This curious behavior can be understood by comparing the results for a sol-gel derived $Al_2O_3-SiO_2:Eu^{3+}$ glass [see Fig. 2(b)], where energy separations increase with an increase in the excitation energy. The main difference between the $SiO_2:Eu^{3+}$ and $Al_2O_3-SiO_2:Eu^{3+}$ glasses is the solubility of the europium ions in each of the glass matrices. It should be noted that SiO_2 glass has a rigid three-dimensional SiO_4 network that limits the solubility of Eu^{3+}. This was also supported by the concentration quenching of fluorescence in the $SiO_2:Eu^{3+}$ glass due to the ion–ion interaction between Eu^{3+} ions. On the other hand, in the $Al_2O_3-SiO_2:Eu^{3+}$ glass, as the con-

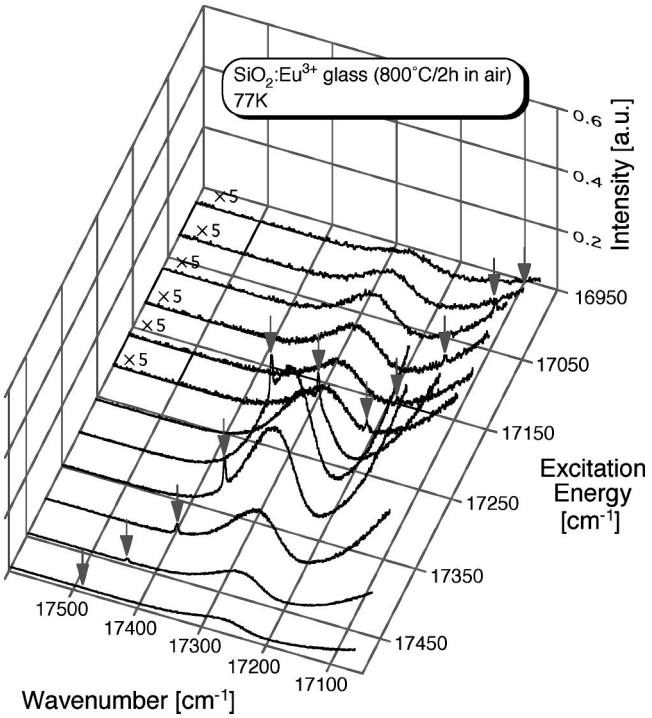

FIG. 3. The fluorescence spectra around a resonant line of the $^5D_0 \rightarrow {}^7F_0$ transition in the SiO_2:Eu^{3+} ($98SiO_2$–$2Eu_2O_3$, 800 °C for 2 h in air; sample A800) for each excitation energy at 77 K. The arrows in the figure show the excitation position.

centration of the Al_2O_3 content increased, Eu^{3+} ions were well dispersed in the glass matrix so that the Eu^{3+} fluorescence was intensified.[33]

Figure 3 shows the fluorescence spectra of sample A800 in the vicinity of a resonant line of the $^5D_0 \rightarrow {}^7F_0$ transition at 77 K. The arrows indicate the location of the resonant lines. Here we see a broad fluorescence band centered at 17 260 cm^{-1} other than the resonant peak on each spectrum. Surprisingly, the shape and peak position of the broadband are not influenced by the excitation energy, and the broadband is capable of being excited with the lower photon energy than its peak energy (17 260 cm^{-1}). In Fig. 4 we depict the peak intensity of the broadband as a function of the excitation energy, which clearly showed the energy structure of a trivalent europium ion as well as the thermal excitation of Eu^{3+} ions at room temperature. Additionally, as the temperature increases, the peak position shifts to the higher energy side and the intensity of the resonant fluorescence concurrently decreases [Fig. 5(a)]. These experimental results lead us to the conclusion that the energy migration among Eu^{3+} ions takes place with the assistance of phonon energy and that the shape of the broadband will approach the inhomogeneous distribution of the $^7F_0 - {}^5D_0$ energy in the glass. Not only sample A1000 but also AV800 has a similar band without the resonant line as depicted in Fig. 5(b), and its temperature dependence is the same as that of sample A800.

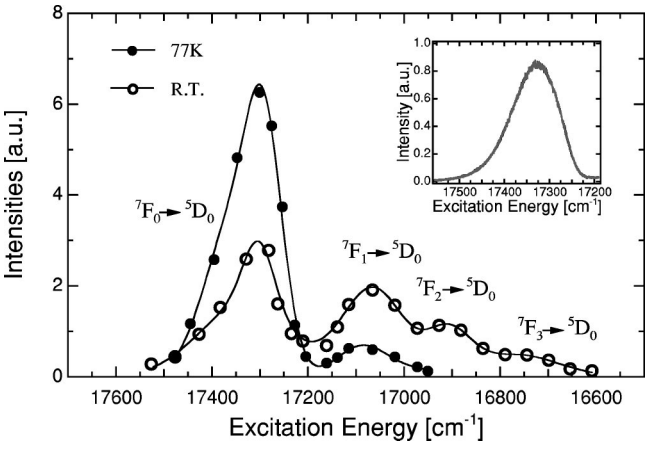

FIG. 4. Excitation spectra of the broad fluorescence band in the $98SiO_2$–$2Eu_2O_3$ glass prepared by the sol-gel method. Insertion shows the excitation spectrum of the $^5D_0 \rightarrow {}^7F_2$ fluorescence in the gel derived Al_2O_3–SiO_2:Eu^{3+} glass. It can also be seen that the Eu^{3+} ions are thermally excited to the $^7F_{1,2,3}$ levels at room temperature.

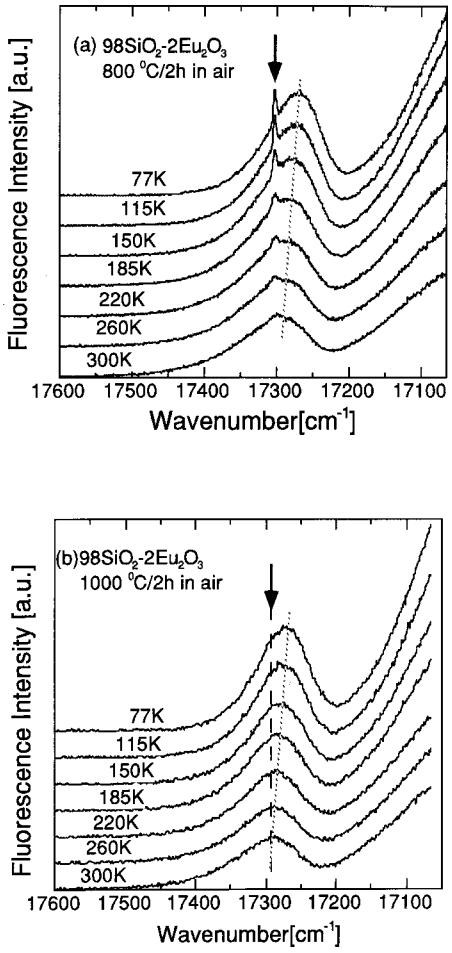

FIG. 5. Temperature-dependence of the broadband around a resonant line of the $^5D_0 \rightarrow {}^7F_0$ transition for (a) sample A800 and (b) A1000. The arrow in the figure stands for the excitation location.

Figure 6 shows decay curves of the $^5D_0 \rightarrow {}^7F_2$ fluorescence for the pulsed excitation to the $^5D_0$ level by the Rhodamine 6G dye laser, which were monitored as time evolutions of the $^5D_0$ population. According to the diffusion model of the excitation energy by Yokota and Tanimoto,[34] a donor fluorescence in energy migration should decay nonexponentially. The donor fluorescence of sample A800 exhibits a slightly nonexponential decay, while the enhanced nonex-

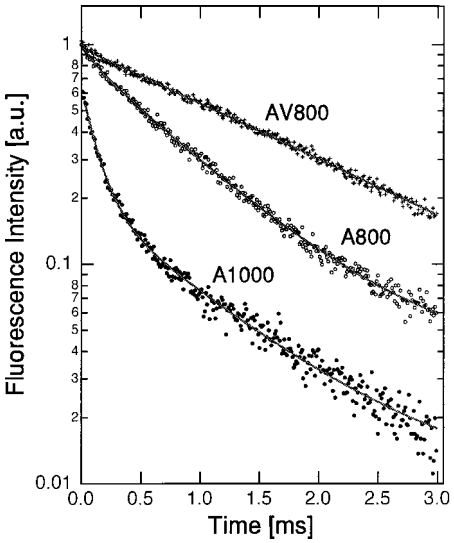

FIG. 6. Fluorescence decay curves of the $^5D_0 \rightarrow {}^7F_2$ transition for the direct excitation to the $^5D_0$ level at room temperature. A dye laser (Rhodamine 6G) pumped by a N_2 laser (pulse width <1 ns) was used as an excitation source.

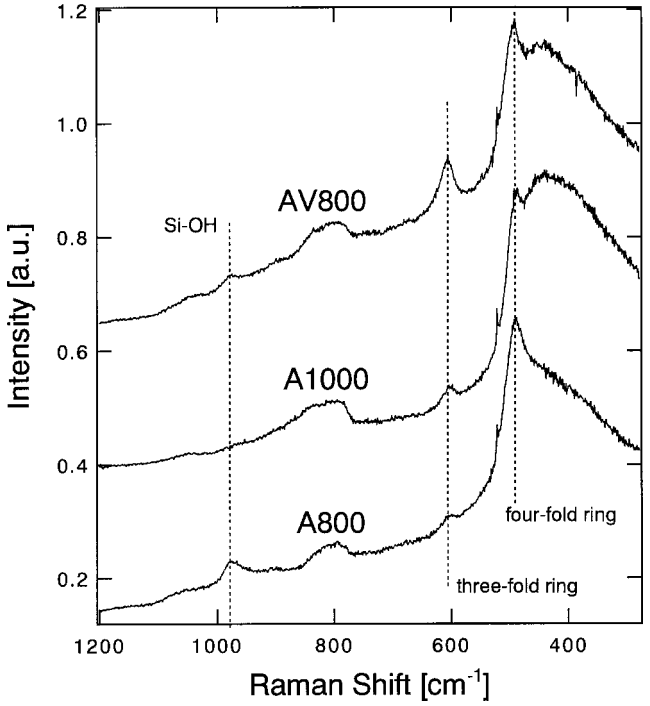

FIG. 7. Raman spectra of $98SiO_2$–$2Eu_2O_3$ glasses prepared by the sol-gel method. The Raman peaks at 405 cm^{-1} (Si–O–Si bending), 800 cm^{-1} (Si–O–Si symmetric stretching), and 1086 cm^{-1} (Si–O–Si asymmetric stretching) are clearly seen (see Ref. 35). The 606 and 485 cm^{-1} Raman peaks correspond to the breathing mode of the planar threefold and fourfold rings, respectively (see Refs. 36 and 37). The peak at 980 cm^{-1} is attributed to the vibration of Si–OH (see Ref. 38).

ponential decay is obtained with sample A1000. Nevertheless, the fluorescence of sample AV800 decays single exponentially. Although both samples A1000 and AV800 had a broadband without the $^5D_0 \rightarrow {}^7F_0$ resonant line, their diffusive behavior of the $^5D_0$ excitation energy is quite different. There must be intrinsic differences between samples A1000 and AV800. It is noted that since the time evolutions after 2 ms are almost the same in all the samples, the initial decays must yield essential information on the diffusion (or migration) processes. The double exponential analysis is summarized in Table I, and its fitting results are also depicted in Fig. 6. Baking of the dry gel at higher temperature produces a reduced lifetime of the initial decay. On the other hand, the initial decay disappears when the obtained glass is subsequently heated in a vacuum.

We also measured the Raman spectra of these samples to investigate their glass structures, which are depicted in Fig. 7. The peak assignment is given in the caption.[35–38] The main structural distinctions are identified by the existence of planar threefold or fourfold rings in 606 or 485 cm^{-1}. The peak at 980 cm^{-1} is attributed to the vibration of Si–OH.

IV. DISCUSSION

In the $10Al_2O_3$–$90SiO_2$:5 wt %Eu_2O_3 glass as depicted in Fig. 8, no prominent broadband in the vicinity of the $^5D_0 - {}^7F_0$ resonant line was observed. The Al-codoping effect on the rare-earth ions embedded in a SiO_2 matrix was investigated by several authors. Arai *et al.*[39] showed that the codopant formed a solvation shell surrounding Nd^{3+} ions to produce a high solubility of the rare-earth ions. Nogami and Abe[33] suggested that an europium ion was preferentially coordinated with a tetrahedral $(AlO_4)^-$ unit in Al_2O_3–SiO_2 glasses derived via the sol-gel route. Laczka[40] reported that the role of rare-earth ions as a network modifier in SiO_2 melt

TABLE I. Fitting parameters in the double exponential analysis for the time-evolutions of $^5D_0$ donor fluorescence under investigation.

Sample	τ_1 (μs)	τ_2 (ms)
A800	415±36	1.23±0.05
A1000	138±3	1.21±0.02
AV800		1.77±0.04

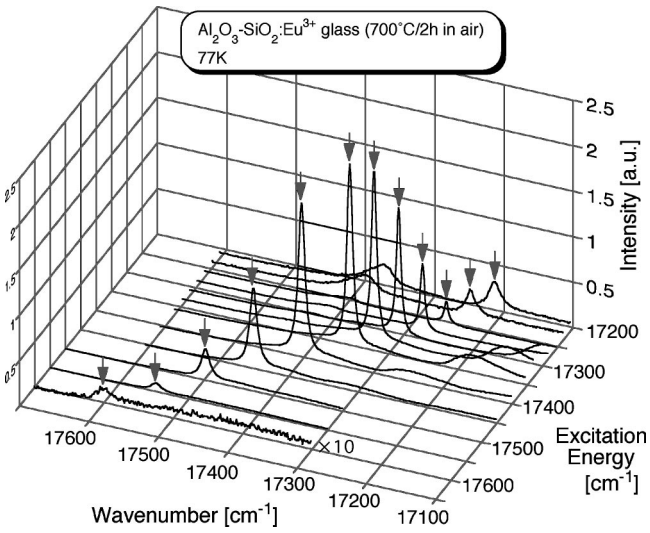

FIG. 8. The fluorescence spectra around a resonant line of the $^5D_0 \rightarrow {}^7F_0$ transition in the Al_2O_3–SiO_2:Eu^{3+} ($10Al_2O_3$–$90SiO_2$:5 wt %Eu_2O_3, 700 °C for 2 h in air) for each excitation energy at 77 K. The arrows in the figure denote the excitation position.

glasses was due to the lower electronegativity versus Si. Considering the experimental results obtained in this study, it is natural to infer that the structural role of rare-earth ions in the sol-gel derived SiO_2 glasses is quite different from that in the melt-quenched SiO_2 glasses, and that the FLN spectra is explained by the existence of an aggregation of Eu^{3+} and O^{2-}, or an Eu–O chemical cluster, in the SiO_2 glass. The strong interactions between Eu^{3+} ions in such an Eu–O chemical cluster, even though the excitation energy was first received by a specific Eu^{3+} ion with line-narrowed irradiation, results in energy migration among the Eu^{3+} sites with the aid of phonon energy.

Yokota and Tanimoto[34] introduced the basic equation for a coexisting system of donor–donor (energy migration) and donor–acceptor (energy trap) transfers with the concept of a ''scattering length method'' and provided insight into the process. Huber *et al.*[41] studied the diffusion process using a fundamental theory based on the microscopic rate equation. The asymptotic behavior of the time evolution of the donor fluorescence for a pulsed excitation is expressed as an exponential function of time with a characteristic lifetime.

$$I/\tau = I/\tau_0 + I/\tau_D, \tag{1}$$

where $1/\tau_0$ is the intrinsic decay rate of the donor level in its isolated system, and $1/\tau_D$ is the decay rate due to diffusion when the donor–acceptor interaction $H_{\mathrm{int}}(r_D - r_A)$ arises from a dipole–dipole coupling and is in the form of $C/(r_D - r_A)^6$,

$$I/\tau_D = 4\pi N_a D \rho, \tag{2}$$

where D is the diffusion constant and N_a is the acceptor concentration. ρ is a length defined by $\rho = 0.68(C/D)^{1/4}$. It can be seen from the above expressions that as the concentration of energy trap N_a or the diffusion constant D increases, the lifetime of the donor fluorescence is reduced (such as was experimentally obtained in the $Eu^{3+}-Cr^{3+}$ system by Weber[42]). Concurrently, it is clearly shown that if the acceptor concentration is significantly low enough to be considered negligible, the decay of the donor fluorescence in energy migrations for the donor–donor system is invariable so as to be characterized only by τ_0.

The thermal treatment at higher temperature in air resulted in the removal of hydroxyl groups and the densification of the gel-glass. The shortening of the first fluorescence decay for the $^5D_0 \rightarrow {}^7F_2$ transition in sample A1000 is attributable to the densification of the gel-glass matrix. As a result, the distance between the Eu^{3+} ions was reduced so that the energy migration process was enhanced. No observation of the resonance line in sample A1000 as shown in Fig. 5(b) gives additional evidence for the extended energy migration. If we assume that the number of energy traps N_a was not a function of the temperature for annealing, the diffusion coefficient D in sample A1000 would be approximately three times greater than in sample A800 (see Table I). It can also be seen that the peak at 980 cm^{-1} was less obvious in samples A1000 and AV800 than in sample A800, indicating the removal of hydroxyl groups from the SiO_2 gel. Nogami *et al.*[43] reported a significant correlation of the burnt hole depth with the content of hydroxyl groups in the sol-gel derived glasses containing Eu^{3+} ions, and proposed a mechanism for the spectral hole burning as an optically induced structural displacement of hydroxyl groups coordinated to Eu^{3+} ions. Since no spectral holes in both A1000 and AV800 were found, the decrease in Si–OH vibration found in the Raman observation is consistent with Nogami's suggestion. The Raman peaks at 485 and 606 cm^{-1} correspond to incomplete structures in the Si–O network. The additional annealing of the SiO_2 glass (A800) in a vacuum produced more threefold ring structures in the resultant glass (AV800). Since the first decay of the donor fluorescence for the $^5D_0$ level suggested the presence of defect centers acting as energy traps (compare the decay curves of A800 and A1000 with that of AV800 in Fig. 6), the annealing in a vacuum might convert such defects into threefold rings. Yet, it is certain that the defect centers of energy traps in the SiO_2 glass are not necessarily associated only with the threefold or fourfold rings observed in the Raman spectra as Galeener suggested.[37]

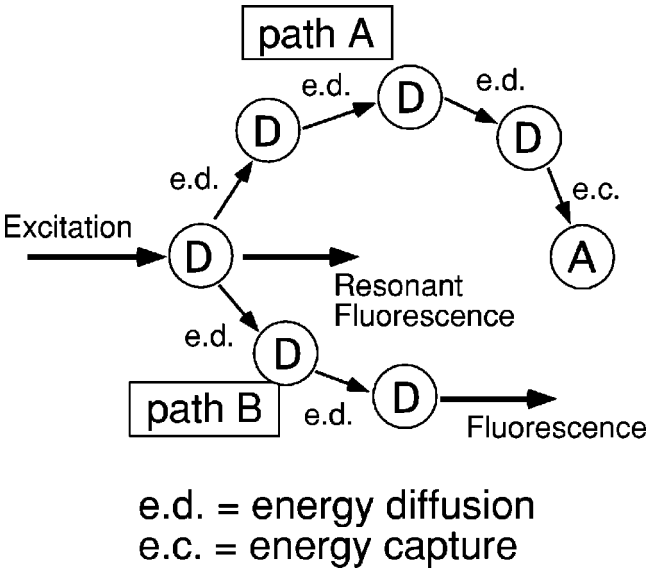

FIG. 9. Two path model for the diffusion process; in paths A and B the energy diffusion takes place as a sequence of phonon-assisted energy transfer. The terminal in path A is an energy trap center (energy acceptor, A), while the energy during migration in path B is emitted as a broadband fluorescence.

From the above discussion it is concluded that two energy paths for the energy migration should be taken into consideration to explain the obtained double exponential decays for the donor ($^5D_0$) fluorescence (see Fig. 9). One is built up by the donor–donor energy migration and subsequent energy trap for a donor–acceptor pair (path A), while the other is the donor–donor migration followed by spontaneous emission (path B) producing the broad fluorescence band in the vicinity of the resonance line. Samples A1000 and AV800 exhibited the extended energy migration due to the reduction of the $Eu^{3+}-Eu^{3+}$ distance with the gel shrinkage. However, the termination of the energy diffusion in path A vanished for sample AV800, resulting in the single exponential decay for the $^5D_0$ fluorescence as shown in Fig. 6.

V. CONCLUSION

The broad fluorescence band in the vicinity of the resonant line of the $^5D_0 \rightarrow {}^7F_0$ transition in the SiO_2 glass produced by the sol-gel method was observed using the FLN technique. Such a remarkable broadband was not observed in the sol-gel derived $Al_2O_3-SiO_2$:Eu^{3+} glass. This indicated energy migration among the Eu^{3+} ions in a Eu–O chemical cluster in the SiO_2 glass. We also measured the time evolution of the fluorescence decay for the $^5D_0 \rightarrow {}^7F_2$ transition, which was explained based on Yokota–Tanimoto's energy diffusion model. It was found that the thermal treatment of the SiO_2:Eu^{3+} gel in air resulted in shrinkage of the SiO_2 matrix and the enhanced energy migration among the Eu^{3+} ions. The diffusion process among the Eu^{3+} ions in the Eu–O chemical cluster could be explained by the following two paths. One was constructed by the energy migration among donors and the subsequent energy trap of a donor–acceptor pair. The other resulted in the spontaneous emission after the donor–donor migration which caused the observed broadband in each of the FLN spectra. Additionally, the subsequent annealing in a vacuum reduced the concentration of energy traps to produce the Raman-active threefold rings in the SiO_2 glass.

ACKNOWLEDGMENTS

T.H. would like to thank Professor Norihiko Kamata of Saitama University and Dr. S. Bharathi of Nagoya Institute of Technology for their fruitful discussions and suggestions. This research was partly supported by a Grant-in-Aid for Scientific Research (No. 13305048 and No. 13026214) from the Ministry of Education, Science, and Culture of Japan.

[1] E. Snitzer, Appl. Opt. **5**, 1487 (1966).
[2] K. Miura, K. Tanaka, and K. Hirao, J. Mater. Sci. Lett. **15**, 1854 (1996).
[3] T. Hayakawa, H. Ooishi, and M. Nogami, Opt. Lett. **26**, 84 (2001).
[4] E. W. J. L. Oomen, J. Non-Cryst. Solids **140**, 150 (1992).
[5] J. Qui, K. Tanaka, N. Sugimoto, and K. Hirao, J. Non-Cryst. Solids **213&214**, 193 (1997).
[6] T. Hayakawa, K. Sato, K. Yamada, N. Kamata, N. Nishi, and F. Maruyama, Synth. Met. **91**, 355 (1997).
[7] T. Hayakawa and M. Nogami, Solid State Commun. **116**, 77 (2000).
[8] K. Hirao, S. Todoroki, D. H. Cho, and N. Soga, Opt. Lett. **18**, 1586 (1993).
[9] K. Hirao, S. Todoroki, K. Tanaka, N. Soga, T. Izumitani, A. Kurita, and T. Kushida, J. Non-Cryst. Solids **152**, 267 (1993).
[10] A. Kurita, T. Kushida, T. Izumitani, and M. Matsukawa, Opt. Lett. **19**, 314 (1994).
[11] S. P. Love, A. J. Sievers, B. L. Halfpap, and S. M. Lindsay, Phys. Rev. Lett. **65**, 1792 (1990).
[12] W. Köhler, J. Zollfrank, and J. Friedrich, J. Appl. Phys. **66**, 3232 (1989).
[13] R. Jaaniso and H. Bill, Europhys. Lett. **16**, 569 (1991).
[14] M. Nogami and Y. Abe, Phys. Rev. B **56**, 182 (1997).
[15] R. Ao, S. Jahn, L. Kümmerl, R. Weiner, and D. Haarer, Jpn. J. Appl. Phys., Part 1 **31**, 693 (1992).
[16] D.-H. Cho, K. Hirao, N. Soga, and M. Nogami, J. Non-Cryst. Solids **215**, 192 (1997).
[17] H. Suzuki, T. Shimada, and H. Hiratsuka, J. Appl. Phys. **70**, 4671 (1991).
[18] M. Mitsunaga, N. Uesugi, H. Sasaki, and K. Karaki, Opt. Lett. **10**, 752 (1994).
[19] M. Nogami and Y. Abe, Appl. Phys. Lett. **71**, 3465 (1997).
[20] M. Nogami and Y. Abe, J. Opt. Soc. Am. B **15**, 680 (1998).
[21] N. Motegi and S. Shionoya, J. Lumin. **8**, 1 (1973).
[22] M. J. Lochhead and K. L. Bray, Mater. Res. Soc. Symp. Proc. **346**, 745 (1994).
[23] Recent progress of PSHB glasses in our laboratory is found in literature; for instance, M. Nogami, T. Hayakawa, and T. Ishikawa, Appl. Phys. Lett. **75**, 3072 (1999); M. Nogami and S. Ito, Phys. Rev. B **61**, 14295 (2000).
[24] P. W. Anderson, Phys. Rev. **109**, 1492 (1958).
[25] D. J. Thouless, J. Phys. C **3**, 1559 (1970).
[26] S. K. Lyo, Phys. Rev. B **3**, 3331 (1971).
[27] S. Chu, H. M. Gibbs, and A. Passner, Phys. Rev. B **24**, 7162 (1981).
[28] C. Brecher and L. A. Riseberg, Phys. Rev. B **13**, 81 (1976); **21**, 2607 (1980).
[29] G. Nishimura and T. Kushida, Phys. Rev. B **37**, 9075 (1988).
[30] M. Tanaka and T. Kushida, Phys. Rev. B **49**, 5192 (1994).
[31] M. Tanaka, G. Nishimura, and T. Kushida, Phys. Rev. B **49**, 16917 (1994).
[32] K. Soga, M. Uo, H. Inoue, A. Makishima, and S. Inoue, J. Am. Ceram. Soc. **78**, 129 (1995).
[33] M. Nogami and Y. Abe, J. Non-Cryst. Solids **197**, 73 (1996).
[34] M. Yokota and O. Tanimoto, Jpn. J. Phys. Soc. **22**, 779 (1967).
[35] C. J. Brinker and G. W. Scherer, in *Sol-gel Science: The Physics and Chemistry of Sol-gel Processing* (Academic, San Diego, CA, 1990), p. 515.
[36] F. L. Galeener, J. Non-Cryst. Solids **49**, 53 (1982).
[37] F. L. Galeener and A. E. Geissberger, Phys. Rev. B **27**, 6199 (1983).
[38] D. M. Krol, C. A. M. Mulder, and J. G. van Lierop, J. Non-Cryst. Solids **86**, 241 (1986).
[39] K. Arai, H. Namikawa, K. Kumata, T. Honda, Y. Ishii, and T. Handa, J. Appl. Phys. **59**, 3430 (1986).
[40] M. Laczka and E. Czerwosz, Glastech. Ber. **61**, 358 (1988).
[41] D. L. Huber, D. S. Hamilton, and B. Barnett, Phys. Rev. B **16**, 4642 (1977).
[42] M. J. Weber, Phys. Rev. B **4**, 2932 (1971).
[43] M. Nogami and T. Hayakawa, Phys. Rev. B **56**, R14235 (1997).